Katrin Weise

STRUCTURE AND MEMBRANE MICRO-DOMAIN LOCALIZATION OF RAS PROTEINS

1 INTRODUCTION

Small GTPases of the rat sarcoma (Ras) superfamily act as binary molecular switches between a GDP-bound inactive and GTP-bound active state and critically regulate numerous biological processes, such as cell proliferation, differentiation, survival, and apoptosis. As peripheral plasma membrane proteins they hold a central position in the transduction of extracellular signals from cell surface receptors across the plasma membrane to intracellular signaling cascades. Mutations in Ras proteins that lead to aberrant signaling are found in approximately 20-30 % of all human cancers [1, 2]. Thereby, mutated Ras is maintained in a constitutively active GTP-bound state and fails to switch off the signal for cell growth.

The highly conserved N-terminal G-domain of Ras encompasses all interaction sites for activators and effectors. Conversely, plasma membrane localization of Ras is directed by the Ras isoform specific C-terminal sequence that constitutes together with the linker domain the hypervariable region (HVR). Ras proteins are posttranslationally modified by alkylation with prenyl moieties and/or acylation with fatty acids. Since non-reversible farnesylation alone confers only limited membrane affinity to Ras proteins, a second, reversible membrane targeting motif, such as one palmitoyl group in case of N-Ras or a polybasic lysine stretch in the 4B splice variant of K-Ras (K-Ras4B), is required to enable anchoring of Ras in the cytoplasmic leaflet of cellular membranes (Fig. 1). The cysteine thioester of the attached palmitoyl group can be hydrolyzed and the polybasic domain partly counterbalanced by phosphorylation of Ser181 within the HVR of K-Ras4B or interaction with acidic proteins such as calmodulin, which led to the postulation of a dynamic spatial cycle for the subcellular localization of N-Ras and K-Ras4B in the cell [3].

Despite interacting with an overlapping set of activators and effectors, the Ras isoforms generate distinct signal outputs *in vivo* and have been proposed to associate with different plasma membrane domains [4-6]. Understanding the lateral
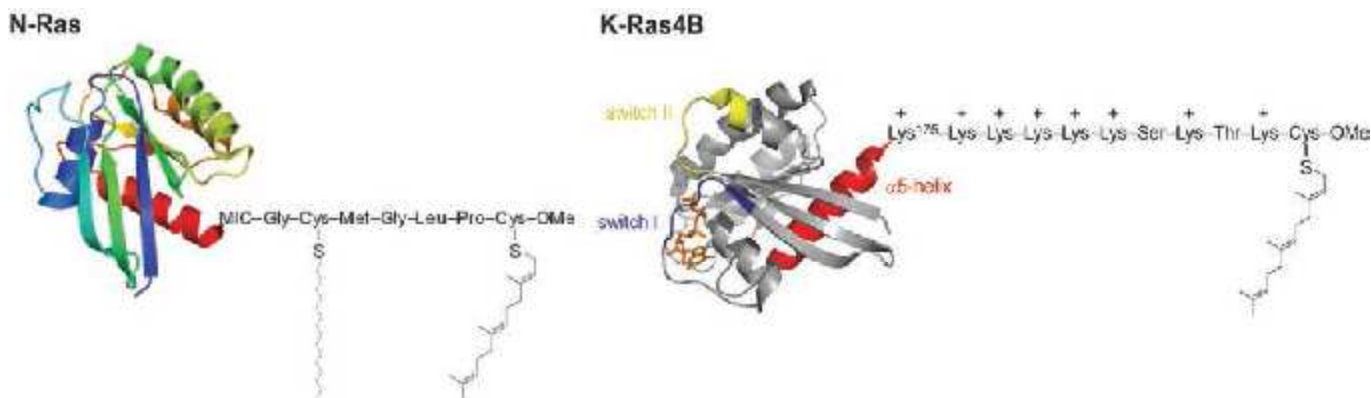
Fig. 1: Schematic representation of the semisynthetic Ras proteins. The membrane anchor is composed of a common C-terminal farnesylated (Far) and carboxymethylated cysteine residue for all Ras isoforms. Whereas K-Ras4B contains a polybasic stretch of six contiguous lysine residues as a second membrane targeting signal, N-Ras bears a palmitoyl chain (replaced by a nonhydrolyzable hexadecyl (HD) group as a palmitoyl analogue in our study). N-Ras HD/Far peptides derivatized at the N-terminus with a maleimidocaproic acid (MIC) amide were coupled to a bacterially expressed, truncated N-Ras protein (amino acid residues 1−181, PDB code: 3CON) carrying a cysteine at the C-terminus. The synthesized, lipidated K-Ras4B peptide was ligated to a truncated K-Ras4B protein expressed in *E.coli* to yield the S-farnesylated K-Ras4B protein bearing an additional cysteine between Gly[174] and Lys[175]. The structure of the G-domain was adapted from the PDB (3GFT) to highlight the switch I region (residues 32-38; blue), switch II region (59-67; yellow), and α5-helix (151-166; red). As a nonhydrolyzable GTP-analogue, the GppNHp-bound state was used. For the fluorescence experiments, the protein core was labeled with BODIPY. Reprinted in part with permission from ref. 16. Copyright 2011 American Chemical Society.

Dr. Katrin Weise
Physikalische Chemie I - Biophysikalische Chemie
Fakultät für Chemie und Chemische Biologie
Technische Universität Dortmund
Otto-Hahn-Straße 6, D-44227 Dortmund, Germany
Tel: +49 (0)231 755 5044
E-Mail: katrin.weise@tu-dortmund.de

organization of the lipid and protein constituents in heterogeneous cellular membranes and the connection between lipid-domain formation and the functional properties of membrane-associated proteins poses one of the major challenging problems in membrane biochemistry and biophysics. There is evidence that distinct regions in cell membranes termed rafts may play a role in a wide range of important biological process-

es, including signal transduction pathways [7, 8]. Such sphingolipids and cholesterol enriched domains could also act as "signaling platforms" that couple events on the outside of the cell with signaling pathways inside the cell. Moreover, recent theoretical and experimental work suggests that the interfacial line tension between domains may play a major role affecting membrane organization [9, 10], but there had been little evidence how this could affect lipoprotein partitioning and nanoclustering in membranes.

In the last years, chemical biology approaches gave access to preparative amounts of fully functional, lipidated Ras proteins by a combination of expressed protein ligation and lipopeptide synthesis [11, 12]. Binding to and lateral organization in heterogeneous model biomembrane systems have been studied for N-Ras and K-Ras4B by a combination of different spectroscopic and imaging techniques. This article summarizes key results obtained recently by our group.

2 LATERAL ORGANIZATION OF RAS PROTEINS IN MODEL BIOMEMBRANES

Model biomembrane systems with three or more lipid components can mimic the matrix of heterogeneous biological membranes. As such, we use a well-established zwitterionic model raft membrane system composed of 1,2-dioleoyl-sn-glycero-3-phosphocholine (DOPC) / 1,2-dipalmitoyl-sn-glycero-3-phosphocholine (DPPC) / Cholesterol (Chol) in a molar ratio of 25:50:25 that segregates into liquid-ordered (l_o, i.e., raft-like) and liquid-disordered (l_d) domains at ambient conditions. To take electrostatic interactions into account that can occur between the positively charged lysines in the K-Ras4B membrane anchor region and negatively charged lipids, a heterogeneous anionic model membrane system was established [13, 14]. Thereby, the zwitterionic model raft mixture was complemented by negatively charged lipids. Incorporation of 10 to 20 mol% phosphatidylglycerol (1,2-dioleoyl-sn-glycero-3-phospho-(1'-rac-glycerol) sodium salt (DOPG) and 1,2-dipalmitoyl-sn-glycero-3-phospho-(1'-rac-glycerol) sodium salt (DPPG)) still leads to liquid phase coexistence at ambient conditions, as shown by atomic force microscopy (AFM) and confocal fluorescence microscopy (Fig. 2).

First, we investigated the interaction of N-Ras with zwitterionic model raft membranes. The results revealed that N-Ras HD/Far proteins were preferentially localized in l_d domains of heterogeneous model membranes. Moreover, they underwent a time-dependent diffusion into and subsequent clustering in the l_o/l_d phase boundary region, independent of GDP/GTP-loading (Fig. 3) [15]. The data provided evidence that the farnesyl anchor is largely responsible for the clustering of N-Ras proteins in the interfacial regions of membrane domains, leading to a decrease of the line energy (tension) between domains. A monofarnesylated N-Ras protein that resembles the depalmitoylated form of the natural N-Ras protein in the course of the acylation/deacylation cycle showed a similar membrane partitioning behavior [15]. Thus, we proposed that the main function of the natural palmitoyl anchor of N-Ras resides predominantly in the residence time in a particular cellular membrane compartment.
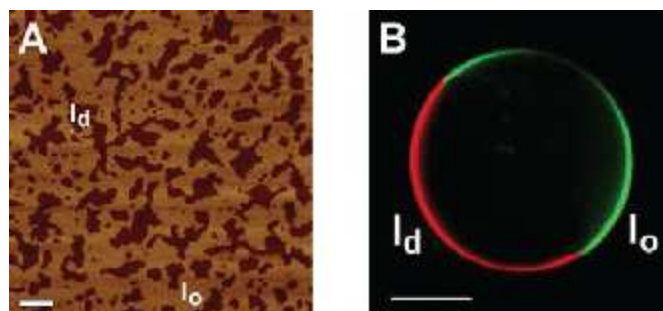
Fig. 2: A) AFM image of a DOPC/DOPG/DPPC/DPPG/Chol 20:5:45:5:25 mol% lipid membrane on mica, indicating a coherent lipid bilayer with coexisting domains. The scale bar corresponds to 1 μm and the vertical color scale from dark brown to white to an overall height of 6 nm. B) Giant unilamellar vesicles (GUVs) were composed of DOPC/DOPG/DPPC/DPPG/Chol 15:10:40:10:25 mol% and showed the round-shaped domains typical for coexisting liquid-like phases. N-(lissamine rhodamine B sulfonyl)-1,2-dihexadecanoyl-sn-glycero-3-phosphoethanolamine triethylammonium salt (N-Rh-DHPE) was used as membrane marker labeling preferentially the l_d domains (red channel); l_o domains were labeled with 23-(dipyrrometheneboron difluoride)-24-norcholesterol (BODIPY-Chol, green channel). The scale bar corresponds to 10 μm.

In contrast to N-Ras, formation of new domains with accumulated protein residing within the bulk l_d phase of the zwitterionic and anionic heterogeneous model membranes was observed for GDP- and GTP-loaded K-Ras4B (Fig. 3) [16]. Thereby, the bulky and branched farnesyl anchor prevents partitioning of K-Ras4B into highly ordered raft-like domains and accommodates more easily into disordered lipid domains. Moreover, formation of the new K-Ras4B enriched domains in the l_d phase of the membrane was shown to be independent on the presence of anionic membrane lipids. Nevertheless, this sorting effect of K-Ras4B is controlled by electrostatic interactions between the positively charged lysines and the negatively charged phosphate of the lipid head groups since the monofarnesylated and non-charged N-Ras revealed a clustering at the lipid domain boundaries under similar conditions [15].

In further studies, the membrane interaction behavior of both N-Ras and K-Ras4B was shown to be independent of the membrane composition [16-18]. Model raft membrane systems of varying degrees of complexity were investigated, leading to the conclusion that even relatively simple heterogeneous model membrane systems are able to reproduce many of the specific properties and functions of membrane-associated proteins in the complex environment of biological membranes.

Taken together, the combined AFM and confocal fluorescence microscopy results led us to propose a molecular mechanism for isoform-specific Ras signaling from separate membrane microdomains [16]. For N-Ras, the expulsion of the protein to the interfacial region combined with a minimization of the line energy between neighboring domains is likely to be one of the key parameters controlling the size and dynamic properties of its signaling platform (Fig. 3, top). Conversely, electrostatic interactions seem to control the membrane interaction process for K-Ras4B. As a consequence, multivalent acidic lipids may be recruited by an effective lipid sorting mechanism and fluid domains with higher anionic charge density and incorporated K-Ras4B protein might be formed (Fig. 3, bottom). For both N-Ras and K-Ras4B no drastic influence of GTP/GDP-loading on the membrane interaction process could be observed. In
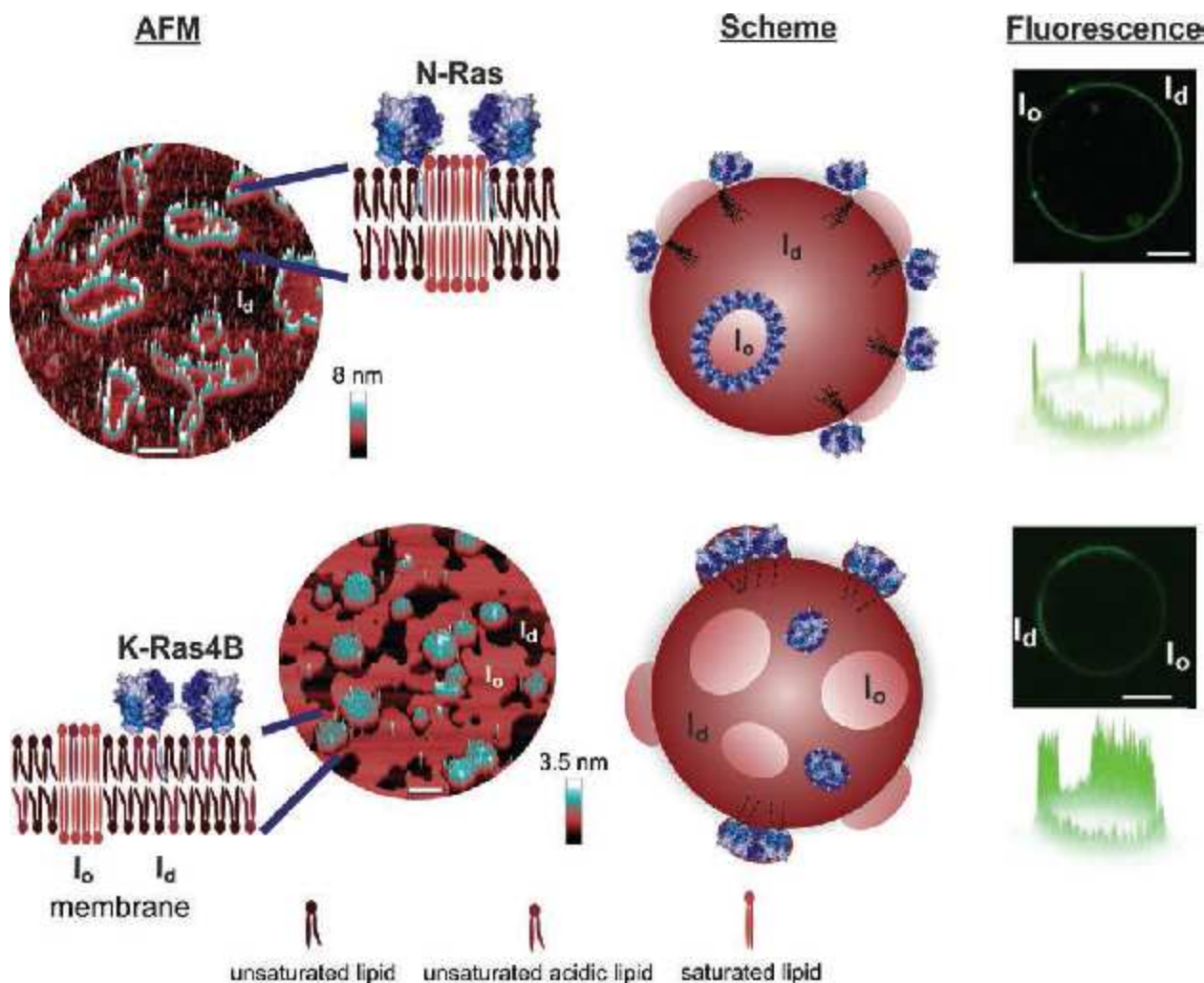
Fig. 3: Postulation of a molecular mechanism for isoform-specific Ras signaling from separate membrane microdomains that could potentially operate as an effective, high fidelity signaling platform with distinct signal outputs for the Ras isoforms: minimization of the line energy (N-Ras) versus lipid sorting through electrostatic interactions (K-Ras4B). N-Ras partitions into the I_d phase of the membrane and subsequently diffuses into the I_d/I_o phase boundaries of the subcompartments as visualized by fluorescence microscopy and AFM (top). In contrast, K-Ras4B forms protein-enriched fluid domains within the bulk I_d phase upon membrane binding and is thought to recruit multivalent anionic lipids by an effective, electrostatic lipid sorting mechanism (bottom). In the 3D AFM images, the clustered proteins are depicted in blue-white and the scale bar corresponds to 1 μm. Superposition of the red (I_d phase, not shown) and green (BODIPY-Ras) channel revealed a localization of the proteins mainly in the I_d phase of heterogeneous membranes, with the fluorescence intensity profiles indicating a significant accumulation of N-Ras in the interfacial region. The scale bar represents 5 μm in both fluorescence microscopy images. Adapted with permission from ref. 16. Copyright 2011 American Chemical Society.

fact, nanoclustering has been proposed in *in vivo* experiments to be critical for signal transmission, as it allows the cell to respond to low signal inputs with a fixed output [19].

3 STRUCTURE AND ORIENTATION OF RAS IN THE PRESENCE OF MEMBRANES

Next to the Ras isoform-specific lateral membrane organization that was shown to be caused by the different Ras membrane anchoring motifs, a possible contribution of the catalytic G-domain to the Ras isoform-specific signal outputs had been addressed. Therefore, conformational and orientational properties of the G-domain of N-Ras and K-Ras4B in their different nucleotide-bound states upon membrane binding were studied using Fourier-transform infrared (FTIR), infrared reflection absorption (IRRA), and polarized attenuated total reflection (ATR) FTIR spectroscopy. The latter was used to examine relative changes in the orientation of GDP- and GTP-loaded N-Ras and

K-Ras4B upon insertion into heterogeneous model membranes [20]. An upward deviation in the dichroic spectrum indicates a transition dipole moment approximately parallel to the membrane normal, whereas a downward deviation designates a preferred alignment of the dipole in the membrane plane. The observed changes in the magnitude of the dichroism implied that, on average, K-Ras4B GTP is more or less randomly orientated, as indicated by the low magnitude of dichroism, presumably due to many different orientations of the G-domain when bound to GTP. Conversely, a strong negative dichroism was detected for K-Ras4B in the inactive form, implying a preferred orientation at the membrane interface (Fig. 4A). Since for the α-helix the stronger component of the amide-I transition dipole is along the helix long axis, negative deviations in the helix region (1648- 1665 cm^{-1}) of the amide-I' band region indicated an orientation of most of the helices in K-Ras4B essentially parallel to the lipid bilayer. Furthermore, differences in the wavenumber maxima of the amide-I' bands suggested differences in the strength of interaction with the membrane, being stronger for

K-Ras4B GDP (amide-I' band maximum at ~1629 cm^{-1}) than for K-Ras4B GTP (amide-I' band maximum at ~1635 cm^{-1}) [20].

For comparison, a preferred orientation with most of the helices oriented essentially parallel to the membrane interface could be inferred from the negative deviations in the helix region of the amide-I' band for N-Ras in both nucleotide-bound states (Fig. 4B). Thereby, slightly stronger membrane interaction was observed for N-Ras GTP (amide-I' maximum at ~1633.5 cm^{-1}) as compared to N-Ras GDP (amide-I' band maximum at ~1637 cm^{-1}). Even though calculation of orientational coordinates from ATR-FTIR data has to be taken with care for Ras

Fig. 4: Orientation of Ras proteins at heterogeneous membranes. A) ATR-FTIR dichroic spectra of K-Ras4B GDP/GTP in the presence of anionic lipid raft membranes composed of DOPC/DOPG/DPPC/DPPG/Chol 20:5:45:5:25 mol%. B) Analogous experiments for N-Ras GDP/GTP in the presence of zwitterionic lipid raft membranes composed of DOPC/DPPC/Chol 25:50:25 mol%. ΔA_N is the absorbance normalized to the sum of the area under the amide-I' band for both the parallel and perpendicular polarized spectra. Reprinted from ref. 20 (Fig. 3) with kind permission from Springer Science and Business Media. Copyright 2012 Springer Science and Business Media.

proteins owing to the fact that in Ras only three of five helices are essentially parallel to each other, there is clear evidence that Ras isoforms adopt conformations with most of the helices in parallel orientation relative to the membrane interface [20].

The Ras G-domain membrane orientation studies were complemented by conducting IRRA spectra at different angles of incidence with p-polarized light and corresponding simulations of the amide-I contour. The results supported the ATR-FTIR data in revealing an, on average, parallel alignment of most of the α- helices relative to the membrane interface for all Ras isoforms, as indicated by a switch in the sign of the IRRA amide-I' signal at an angle of incidence above the Brewster angle. In addition, an inverted interaction profile was obtained for K-Ras compared with N-Ras. Whereas the active conformation of N-Ras seemed to exhibit an interaction with the membrane that is mediated by the α4/5-helices, K-Ras4B displayed a higher flexibility in the active state, where the α4-helix does not seem to directly interact with the membrane [20, 21]. The weaker interaction and higher reorientational flexibility of active K-Ras4B at the membrane interface was further confirmed by corresponding transmission FTIR experiments. However, the secondary structure of K-Ras4B was not significantly affected upon binding to heterogeneous membranes [16].

Taken together, the infrared spectroscopic results led to the conclusion that Ras isoform specificity extends beyond the HVR to the highly conserved G-domain. Thereby, the G-domain mediates Ras-membrane interaction by inducing different sets of preferred orientations in the active and inactive state. Hence, Ras isoform specificity might be further determined by different degrees of orientational flexibility for the active and inactive state of Ras, which might be important for isoform-specific effector interactions [20].

4 REGULATION OF RAS MEMBRANE LOCALIZATION

The GDI-like solubilizing factor GMP phosphodiesterase 6 delta subunit (PDEδ) has been proposed to function as a cytoplasmic prenyl binding factor and accordingly is supposed to assist in the intracellular trafficking and proper signaling of Ras [22, 23]. By shielding the hydrophobic anchor (particularly farnesyl) from the cytosol, PDEδ would facilitate intracellular Ras diffusion and allow Ras proteins to shuttle between cellular membranes. Recent results revealed an essential role of PDEδ for the plasma membrane localization of K-Ras4B, whereby the Arl2-PDEδ perinuclear membrane delivery system seems to regulate a dynamic spatial cycle of K-Ras4B in the cell [24-26]. The hydrophobic pocket of PDEδ binds and solubilizes farnesylated K-Ras4B proteins irrespective of the bound nucleotide state [24, 26]. Although a PDEδ-mediated extraction of membrane-anchored Ras proteins from cellular membranes was proposed [23, 27], no direct molecular-level evidence for such a mechanism could be obtained until lately.

By using a combination of different biophysical techniques we studied the interaction of GDP- and GTP-bound K-Ras4B with PDEδ in the absence and presence of heterogeneous model membranes [28]. Surface plasmon resonance (SPR) experiments re-

vealed that PDEδ is not able to extract K-Ras4B from membranes, independent of membrane composition and nucleotide loading since the amount of membrane-bound K-Ras4B and hence the SPR signal is not reduced by the addition of PDEδ (Fig. 5A). Instead, PDEδ binds to the membrane itself. To further characterize the interaction of GDP- and GTP-loaded K-Ras4B with PDEδ and heterogeneous membranes, frequency-domain fluorescence anisotropy was used. According to the (rotational) Stokes-Einstein relation, the rotational correlation time, $\theta_{protein}$, determined experimentally is proportional to the size (hydrodynamic volume) of the fluorescent protein, i.e., the BODIPY-labeled K-Ras4B. Whereas a truncated control protein (K-Ras4B GDP trunc.) that lacked the farnesyl anchor showed no binding to PDEδ, an almost doubling of the overall rotational correlation time was observed upon addition of PDEδ to K-Ras4B GTP in aqueous buffer solution due to

complex formation of the nearly equally sized proteins. Further addition of lipid vesicles composed of the anionic lipid raft mixture to the K-Ras4B/PDEδ complex did not significantly alter the rotational dynamics of K-Ras4B (Fig. 5B).

To investigate whether or not the K-Ras4B/PDEδ complex stayed intact and interacted with the membrane, IRRAS and AFM experiments were carried out. Thereby, the surface pressure profile, i.e., π in dependence on the time t after protein injection, was indicative of an effective insertion of the farnesyl anchor of K-Ras4B into the anionic lipid monolayer, which led to a marked increase in surface pressure with proceeding membrane insertion. In contrast to K-Ras4B, when adding PDEδ only, the surface pressure profile revealed the absence of significant insertion. Finally, the π/t profile of the K-Ras4B GTP/PDEδ com-
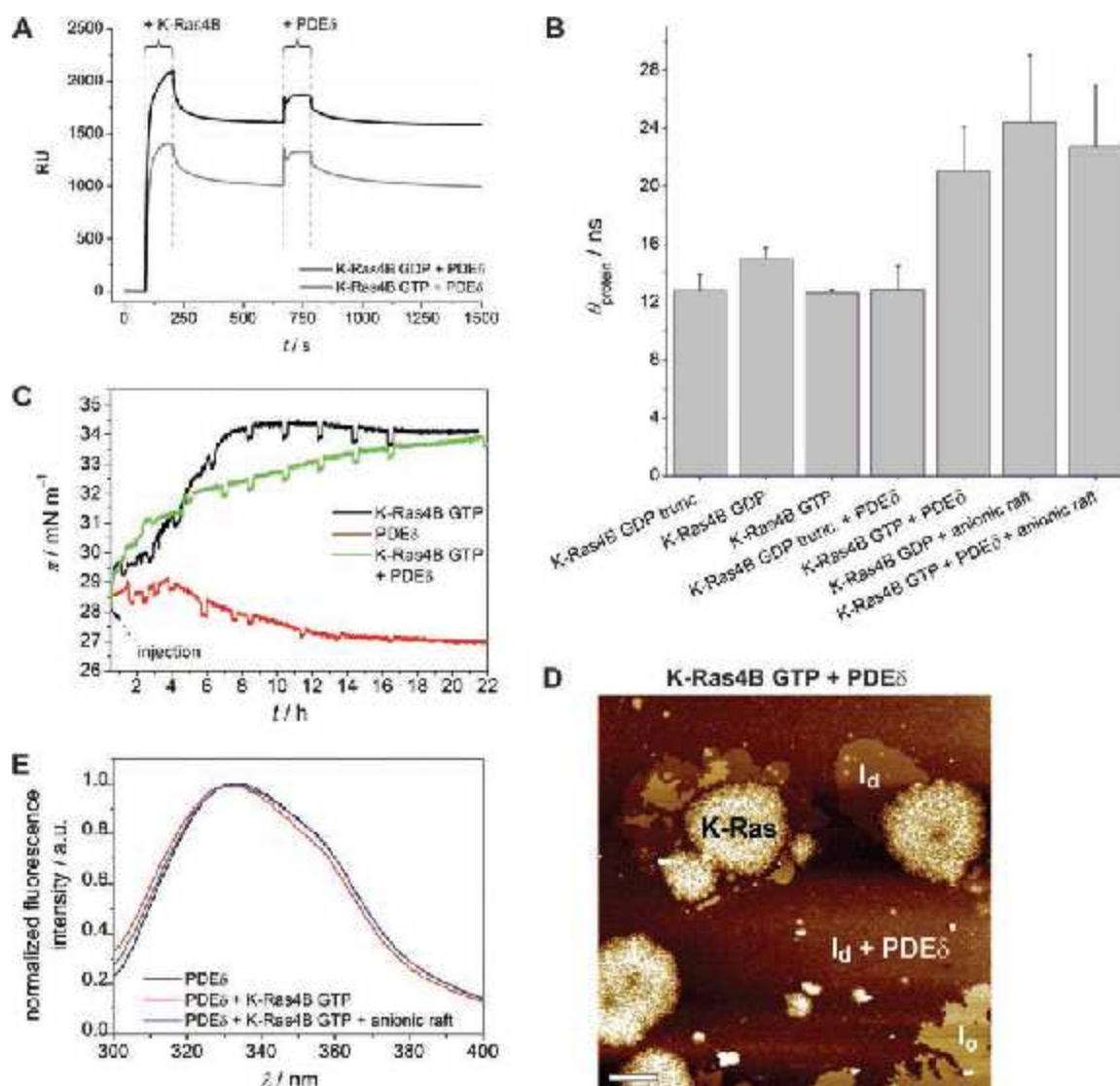
Fig. 5: A) SPR sensorgrams comprise a plot of the SPR signal in resonance units (1 RU = 1 pg mm^{-2}, i.e., surface coverage with protein in terms of mass protein/mm^2 surface area) against time and show the binding of GDP- and GTP-loaded K-Ras4B to anionic model raft membranes as well as subsequent addition of PDEδ. B) Overall rotational correlation times of BODIPY-labeled K-Ras4B at T = 25° C. Results are shown for GDP- and GTP-loaded K-Ras4B in the presence and absence of PDEδ and/or heterogeneous model raft membranes. C) Surface pressure profiles for K-Ras4B GTP, PDEδ, and the preformed K-Ras4B GTP/PDEδ complex upon interaction with the anionic lipid raft monolayer. The dips are due to shuttling between the reference and sample trough when the corresponding IRRA spectra are collected. D) The AFM image of the interaction of the preformed K-Ras4B/PDEδ complex with anionic raft membrane displays the membrane partitioning at a representative time point after injection of protein solution into the AFM fluid cell. The overall height of the vertical color scale from dark brown to white corresponds to 6 nm; the scale bar represents 1 μm. E) Normalized fluorescence spectra of PDEδ in bulk solution (black), the K-Ras4B GTP/PDEδ complex in bulk solution (red), and the complex upon interaction with the anionic raft membrane (blue). The spectra show the change of the PDEδ tryptophan emission maximum and band shape upon complexation and membrane-mediated dissociation of the PDEδ and K-Ras4B GTP complex. Adapted with permission from ref. 28. Copyright 2012 American Chemical Society.

plex preformed in bulk solution resembled that of the active K-Ras4B monolayer interaction, that is, the insertion of K-Ras4B GTP into the lipid monolayer. This led to the assumption that the K-Ras4B GTP/PDEδ complex dissociates upon membrane contact, releasing the lipid anchor of K-Ras4B for membrane insertion (Fig. 5C). Complementary AFM measurements of the preformed K-Ras4B GTP/PDEδ complex confirmed this finding in showing AFM images that mirrored the membrane partitioning behavior of the single components. This means that both, domains with accumulated K-Ras4B GTP protein inside a fluid-like environment as well as homogeneously distributed PDEδ in a thinned l_d phase were detected (Fig. 5D). The same results were obtained for comparative experiments performed with inactive K-Ras4B and zwitterionic model raft membranes [28].

To directly prove the dissociation of the K-Ras4B/PDEδ complex upon membrane interaction, the emission spectra of PDEδ can be monitored in the absence and presence of K-Ras4B and heterogeneous membranes. When K-Ras4B binds to PDEδ by insertion of its farnesyl anchor into the hydrophobic binding pocket of PDEδ, a blue shift to lower wavelengths was observed in the fluorescence spectra. This is indicative for a decrease in the polarity of the fluorophor's surroundings, which corresponds mainly to residues Tyr149 and Trp32 being involved in or closely related to the hydrophobic binding pocket of PDEδ, respectively. When lipid vesicles composed of the anionic raft mixture were added to the K-Ras4B GTP/PDEδ complex, the initial fluorescence spectrum of PDEδ was recovered, arguing for a dissociation of the farnesyl from the binding pocket of PDEδ (Fig. 5E).

To conclude, the combined results revealed that PDEδ is not able to extract membrane-bound K-Ras4B, irrespective of nucleotide-loading and membrane composition. This can be explained by the lack of exposed binding sites for PDEδ when K-Ras4B is anchored in membranes, because binding of PDEδ to K-Ras4B occurs only through the farnesylated C-terminus of K-Ras4B. The determined enhanced affinity of the K-Ras4B/PDEδ complex particularly to anionic membranes together with the observation that K-Ras4B is released from PDEδ upon membrane interaction led us to propose an effective delivery of PDEδ-solubilized K-Ras4B to the plasma membrane [28]. These findings are in agreement with a current work, showing that binding of K-Ras4B to PDEδ is a passive sequestration in the cytoplasm of dissociated K-Ras4B from any membrane [25]. Thus, PDEδ sustains the spatial organization of K-Ras4B in cells by enriching K-Ras4B at the plasma membrane for augmented signaling.

5 FROM ARTIFICIAL TO NATURAL PLASMA MEMBRANE SYSTEMS

Although the interaction of both N-Ras and K-Ras4B with model raft membrane systems of varying degrees of complexity had been shown to be independent of the membrane composition [16-18], data on the effect of natural plasma membranes with and without membrane proteins on the membrane partitioning of Ras are still largely missing. Giant plasma membrane vesicles (GPMVs) serve as ideal models of natural membrane systems as they are directly released from the cell plasma membrane by chemically induced blebbing of mammalian cells [29, 30]. There-

by the cellular plasma membrane lipid and protein composition is preserved, thus closing the gap between artificial and cellular membrane system. To gain insight into the Ras membrane interaction process in the complex milieu of the plasma membrane, a protocol for a biological plasma membrane system was established by our group that exhibits fluid phase separation at physiological temperature and hence enables subsequent protein partitioning studies using a variety of biophysical techniques [31]. In particular, the lipid phase behavior of protein containing GPMVs isolated from RBL-2H3 cells was compared to that of the corresponding GPMV lipid extracts that were reconstituted as protein-depleted vesicles. The data revealed an ordering effect of membrane proteins on the lipid system at temperatures below 25 °C and pointed toward a higher overall conformational order of these complex natural membranes in their all-fluid-like state. However, observed differences between coexisting phases of the two membrane systems were small, i.e., even plasma membrane protein levels of ~40% (w/w) had no drastic effect on the lipid phase behavior of the GPMV system [31].

To this end, preliminary data indicate that both N-Ras and K-Ras4B partition into liquid-disordered phases even in the complex milieu of natural plasma membranes. This finding suggests that plasma membrane proteins do not significantly alter the plasma membrane localization of Ras.

6 CONCLUSION

The Ras oncoproteins most frequently found in human tumors are activated K-Ras4B and N-Ras. Recent work hypothesized that Ras plasma membrane localization is dynamically maintained by a spatially organizing cycle [3]. For K-Ras4B, this localization cycle is thought to be modulated by posttranslational modifications of K-Ras4B, such as phosphorylation, and cytosolic solubilizing factors, such as PDEδ. Interference in K-Ras4B plasma membrane localization would constitute a possibility to impact cell growth and counter oncogenic K-Ras4B signaling, since the signaling activity of Ras is intrinsically tied to its level of enrichment at the plasma membrane.

REFERENCES

[1]   Bos, J. L. *Cancer Res.* 1989, **49**, 4682–4689.

[2]   Prior, I. A.; Lewis, P. D.; Mattos, C. *Cancer Res.* 2012, **72**, 2457–2467.

[3]   Schmick, M.; Kraemer, A.; Bastiaens, P. I. H. *Trends Cell Biol.* 2015, **25**, 190–197.

[4]   Parton, R. G.; Hancock, J. *Trends Cell Biol.* 2004, **14**, 141–147.

[5] Prior, I. A.; Muncke, C.; Parton, R. G.; Hancock, J. F. *J. Cell Biol.* 2003, **160**, 165–170.

[6] Plowman, S. J.; Ariotti, N.; Goodall, A.; Parton, R. G.; Hancock, J. F. *Mol. Cell Biol.* 2008, **28**, 4377–4385.

[7] Omerovic, J.; Prior, I. A. *FEBS J.* 2009, **276**, 1817–1825.

[8] Simons, K.; Toomre, D. *Nat. Rev. Mol. Cell Biol.* 2000, **1**, 31–41.

[9] Kuzmin, P. I.; Akimov, S. A.; Chizmadzhev, Y. A.; Zimmerberg, J.; Cohen, F. S. *Biophys. J.* 2005, **88**, 1120‑1133.

[10] Garcia-Sáez, A. J.; Chiantia, S.; Schwille, P. *J. Biol. Chem.* 2007, **16**, 33537‑33544.

[11] Bader, B.; Kuhn, K.; Owen, D. J.; Waldmann, H.; Wittinghofer, A.; Kuhlmann, J. *Nature* 2000, **403**, 223–226.

[12] Chen, Y.-X.; Koch, S.; Uhlenbrock, K.; Weise, K.; Das, D.; Gremer, L.; Brunsveld, L.; Wittinghofer, A.; Winter, R.; Triola, G.; Waldmann, H. *Angew. Chem. Int. Ed.* 2010, **49**, 6090–6095.

[13] Kapoor, S.; Werkmuller, A.; Denter, C.; Zhai, Y.; Markgraf, J.; Weise, K.; Opitz, N.; Winter, R. *Biochim. Biophys. Acta* 2011, **1808**, 1187–1195.

[14] Evers, F.; Jeworrek, C.; Weise, K.; Tolan, M.; Winter, R. *Soft Matter* 2012, **8**, 2170–2175.

[15] Weise, K.; Triola, G.; Brunsveld, L.; Waldmann, H.; Winter, R. *J. Am. Chem. Soc.* 2009, **131**, 1557–1564.

[16] Weise, K.; Kapoor, S.; Denter, C.; Nikolaus, J.; Opitz, N.; Koch, S.; Triola, G.; Herrmann, A.; Waldmann, H.; Winter, R. *J. Am. Chem. Soc.* 2011, **133**, 880–887.

[17] Vogel, A.; Reuther, G.; Weise, K.; Triola, G.; Nikolaus, J.; Tan, K.-T.; Nowak, C.; Herrmann, A.; Waldmann, H.; Winter, R.; Huster, D. *Angew. Chem. Int. Ed.* 2009, **48**, 8784–8787.

[18] Vogel, A.; Nikolaus, J.; Weise, K.; Triola, G.; Waldmann, H.; Winter, R.; Herrmann, A.; Huster, D. *Biol. Chem.* 2014, **395**, 779–789.

[19] Tian, T.; Harding, A.; Inder, K.; Plowman, S.; Parton, R. G.; Hancock, J. F. *Nature Cell Biol.* 2007, **9**, 905–914.

[20] Kapoor, S.; Weise, K.; Erlkamp, M.; Triola, G.; Waldmann, H.; Winter, R. *Eur. Biophys. J.* 2012, **41**, 801–813.

[21] Kapoor, S.; Triola, G.; Vetter, I. R.; Erlkamp, M.; Waldmann, H.; Winter, R. *Proc. Natl. Acad. Sci. U. S. A.* 2012, **109**, 460–465.

[22] Hanzal-Bayer, M.; Renault, L., Roversi, P.; Wittinghofer, A.; Hillig, R. C. *EMBO J.* 2002, **21**, 2095‑2106.

[23] Nancy, V.; Callebaut, I.; El Marjou, A.; de Gunzburg, J. *J. Biol. Chem.* 2002, **277**, 15076–15084.

[24] Chandra, A.; Grecco, H. E.; Pisupati, V.; Perera, D.; Cassidy, L.; Skoulidis, F.; Ismail, S. A.; Hedberg, C.; Hanzal-Bayer, M.; Venkitaraman, A. R.; Wittinghofer, A.; Bastiaens, P. I. H. *Nat. Cell Biol.* 2011, **14**, 148–158.

[25] Schmick, M.; Vartak, N.; Papke, B.; Kovacevic, M.; Truxius, D. C.; Rossmannek, L.; Bastiaens, P. I. H. *Cell* 2014, **157**, 459–471.

[26] Ismail, S. A.; Chen, Y.-X.; Rusinova, A.; Chandra, A.; Bierbaum, M.; Gremer, L.; Triola, G.; Waldmann, H.; Bastiaens, P. I. H.; Wittinghofer, A. *Nat. Chem. Biol.* 2011, **7**, 942–949.

[27] Bhagatji, P.; Leventis, R.; Rich, R.; Lin, C.-j.; Silvius, J. R. *Biophys. J.* 2010, **99**, 3327–3335.

[28] Weise, K.; Kapoor, S.; Werkmüller, A.; Möbitz, S.; Zimmermann, G.; Triola, G.; Waldmann, H.; Winter, R. *J. Am. Chem. Soc.* 2012, **134**, 11503–11510.

[29] Scott, R. E. *Science* 1976, **194**, 743–745.

[30] Baumgart, T.; Hammond, A. T.; Sengupta, P.; Hess, S. T.; Holowka, D. A.; Baird, B. A.; Webb, W. W. *Proc. Natl. Acad. Sci. U. S. A.* 2007, **104**, 3165–3170.

[31] Seeliger, J.; Erwin, N.; Rosin, C.; Kahse, M.; Weise, K.; Winter, R. *Phys. Chem. Chem. Phys.* 2015, **17**, 7507–7513.